Regular Article

ANALYTICAL AND BIOANALYTICAL CHEMISTRY RESEARCH

Published by the Iranian Chemical Society

Anal. Bioanal. Chem. Res., Vol. 7, No. 1, 111-129, January 2020.

Naked Eye Chemosensor for the Qualitative and Quantitative Determination of Oxalate Ions Based on Indicator Displacement Assay

Amin Hemmati Yadkoori, Habibollah Khajehsharifi*, Ardeshir Shokrollahi and Mohammad Mahdi Bordbar

Department of Chemistry, Yasouj University, Under Hill, Yasouj, Iran

(Received 20 October 2018 Accepted 6 August 2019)

Herein, a simple, sensitive, and rapid chemosensor is reported for the colorimetric detection and determination of oxalate ions. This system produces a visible color change from purple to yellow based on the indicator displacement assay (IDA) approach. The reaction of Eriochrome Cyanine R (ECR) as an indicator and vanadyl ions (VO^{2+}) at pH 6.00 acts as a chemosensor for oxalate ions (Ox). Adding oxalate ions to the designed chemosensor causes the replacement of the vanadyl ions with the oxalate ions to binding the indicator. Due to this displacement, the solution color returns to yellow with about 80 nm blue shifts (530 to 450 nm). Also, the formation constants of ECR-VO^{2+} and VO^{2+}-Ox complexes were determined to be 6.13 and 13.94, respectively using spectrophotometric titration. Under the optimized experimental conditions, the chemosensor exhibited a dynamic linear range for oxalate ions from 8.30×10^{-7}-1.13×10^{-4} M, with a detection limit (S/N = 3) of 5.40×10^{-7} M. The relative standard deviation (RSD) value was evaluated to be 0.52% for five determinations of oxalate (6.02 μM). The designed sensor was applied successfully for the determination of oxalate ions in human urine samples with the recoveries of 96.36 to 105.73% showing satisfactory results.

Keywords: Chemosensing ensemble, Oxalate, Vanadyl, Eriochrome cyanine R

INTRODUCTION

Oxalate in the human body is produced by metabolism of protein, but high concentrations of oxalate ions are toxic due to the production of insoluble complexes with some cations [1]. The existence of the oxalate in the urine usually indicates the kidney stones. Thus the measurement of oxalate ions is very important in detecting kidney stones and many other diseases. For example, inordinate generation and excretion of oxalate in the urine cause the impaired conversion of glyoxalate to glycine resulting in a metabolic disease called hyperoxaluria [2]. Oxalate is often found in the herbal foods. Excessive consumption of the oxalate containing vegetables like spinach, chard and okra also can cause kidney stones. On the other hand, oxalic acid interferes with iron absorption reduces its cotribution in body.

Because of combining calcium with oxalate ions in the gut, oxalate stones are produced results in lack of calcium in the gut; so large amounts of the oxalate gos to the kidneys for excretion from the body. Normal men and women excrete 17 to 43 mg oxalic acid per day [3].

With measuring the urine and plasma oxalate contents, some of the disorders are identified such as urinary stones, malabsorption, steatorrhoea, ileal disease, and ethylene glycol poisoning.

The identification and determination of ions using the sensors consisting of pure H- bonding sites is difficult in aqueous media [4], because the anions have to compete with a solvent for H-bonding sites of chemosensors [5]. Lately, metal complexes with an indicator were used for the sensing of anions [6].

There are few methods for the measurement of oxalate, including indirect absorption spectrometry [7], indirect

*Corresponding author. E-mail: khajeh_h@yahoo.com

fluorometric [8], immobilizing oxalate oxidase [9], complexation method [10], gas chromatography [11], enzymatic method [12-14], HPLC [15,16] and ion chromatography [17,18]. Some of the mentioned methods are time consuming (*e.g*., chromatography and electrochemistry) and some others need sample pre-treatments. Also, these methods need multiple sample parameters and high levels of blood or urine [19-22].

Some of the oxalate biosensors disadvantages are: a) Leaking out of bio elements, enzymes and chemicals; b) Immobilization of oxalate oxidase onto the transducer which must be as strong as possible; c) Fabrication of biosensors that can reproduce the results with uniformity; d) Selectivity and detection range which can be more selective and wide domain [23].

The chemical sensor is a sensorial receptor converting chemical signals to the action potential. This sensor can be used for the economical and rapid oxalate analysis in urine, plasma and foodstuff. Also, nowadays using IDA method has been developed for the detection and identification of different analytes. An indicator binds with an acceptor. Then, the analyte is entered into the system and replaced with the indicator to bind to the metal ions showing analyte high affinity for binding to the host (Fig. 1). The indicator displacement assay has been greatly noticed by researchers for their rapidity, selectivity, sensitivity, stability and repeatability [24-26].

In earlier years, easy monitoring of the UV-Vis or fluorescence signals (as output) through a variety of molecular logic gates based on absorption or emission behavior of the chemosensors has been attracted considerable attention [27-32]. Logic gates are the apparatus used to make basic logic operations. The first time logic gates were implemented at molecular level by Ari Aviram in 1988 [33] and were extended by De Silva [34]. In Table 1, a variety of logic gates are presented. These logic gates are NOT, AND, NAND, OR, NOR, XOR and XNOR which can be used in chemical sensors with corresponding truth tables.

Changes in absorption and emission properties of the chemosensors can be presented with Boolean algebra with two levels which called ‘on’ and ‘off’ or ‘1’ and ‘0’ states for high and low levels or signals, respectively. In the chemosensing method, these logic gates produce colorimetric or fluorescent signals as outputs from the chemical inputs.

Herein, a simple, fast and convenient colorimetric sensor (ECR-Vanadyl complex solution) was designed successfully for the detection and determination of oxalate ion in the aqueous solution based on the IDA approach. Also, by using Vanadyl and oxalate ions as chemical inputs and the absorbance intensity of the oxalate as output, the corresponding logic gate of this system was determined to be XNOR to accommodate with the miniaturization of the procedure information.

EXPERIMENTAL

Chemicals

All the chemicals were of analytical grade and purchased from Merck Company. The stock solutions of ECR, vanadyl ions and sodium oxalate (1.00×10^{-3} M) were prepared daily by dissolving their appropriate amount in double distilled water. The acetic acid–ammonia buffer (pH = 6.00) was selected as an appropriate buffer solution [35]. The stock solution of glacial acetic acid was provided and adjusted to the desired pH with ammonia solution. The concentrations of the solutions were prepared by diluting their stock solutions. Throughout the experiments, double distilled water was used.

Instruments

UV-Vis absorbance measurements were carried out by a Perkin Elmer-Lambda 25 spectrometer in a 10 mm path length quartz cuvette. An AZ instrument Corps model 86502 pH-meter was used to measure pH. H-NMR spectra were recorded using Bruker instruments NMR (400 MHz). All the measurements were performed at room temperature.

General Procedure

In this indicator displacement assay system, vanadyl ions and ECR were employed respectively as a receptor and colorimetric indicator for the determination of oxalate ions. The interaction between VO^{2+} and ECR was investigated from a spectrophotometric titration. Then, oxalate ions were added to this complex solution (chemosensor) then titrated with oxalate ions.

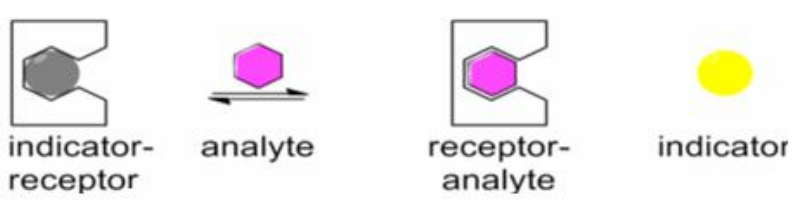

Fig. 1. Schematic of the indicator displacement assay.

Table 1. Sorts of the Logic Gates with the Symbols and Truth Table [40]

Logic Gates

Name	NOT	AND	NAND	OR	NOR	XOR	XNOR
Alg. Expr.	$\overline{A}$	AB	$\overline{AB}$	$A+B$	$\overline{A+B}$	$A \oplus B$	$\overline{A \oplus B}$
Symbol	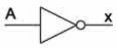	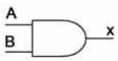					
Truth Table	A X 0 1 1 0	B A X 0 0 0 0 1 0 1 0 0 1 1 1	B A X 0 0 1 0 1 1 1 0 1 1 1 0	B A X 0 0 0 0 1 1 1 0 1 1 1 1	B A X 0 0 1 0 1 0 1 0 0 1 1 0	B A X 0 0 0 0 1 1 1 0 1 1 1 0	B A X 0 0 1 0 1 0 1 0 0 1 1 1

The change of solution color to its primary color refers to the release of indicator dye and the complexation between vanadyl and oxalate ions. The displacement of ECR with the oxalate is due to stronger binding of VO^{2+}-Ox than that of ECR-VO^{2+}. So, the designed colorimetric chemosensor acts via the IDA procedure; also, it is the naked eye chemosensor because this process is accompanied by a change in color from purple to yellow. Using the Job's method for ECR-VO^{2+} and VO^{2+}-Ox complexes, stoichiometric ratios of 1:1 and 2:1 are confiremnd for ECR-VO^{2+} and VO^{2+}-Ox complexes. The association constants of ECR-VO^{2+} and VO^{2+}-Ox complexes show a more tendency of oxalate ions to bind to vanadyl ion than ECR. The process, in summary, can be shown in the following equations:

$$ECR + V(IV) = ECR{:}V \quad (1)$$

$$ECR{:}V(IV) + 2Ox = V\,(IV){:}2Ox + ECR \quad (2)$$

RESULTS AND DISCUSSION

The pH Effect

The pH plays an essential role in the interaction of ECR-VO^{2+} andVO^{2+}-Ox complexes. The change in the absorbance of ECR-VO^{2+} and ECR-VO^{2+}-Ox complexes were investigated in 450 and 530 nm as a function of pH changes of the solution. The designed sensor response at several pH values from 3.00 to 12.00 was investigated for optimizing its pH (Fig. 2). As pH was increased to 6.00, the sensor response increased towards oxalate ions and vanadyl -oxalate complex. Thus, pH 6.00 was selected as the optimum pH, which is in agreement with previous reports [36]. At pH < 6.00, vanadyl ions compete with hydrogen ions to occupy binding sites of the ligand. Also, at acidic

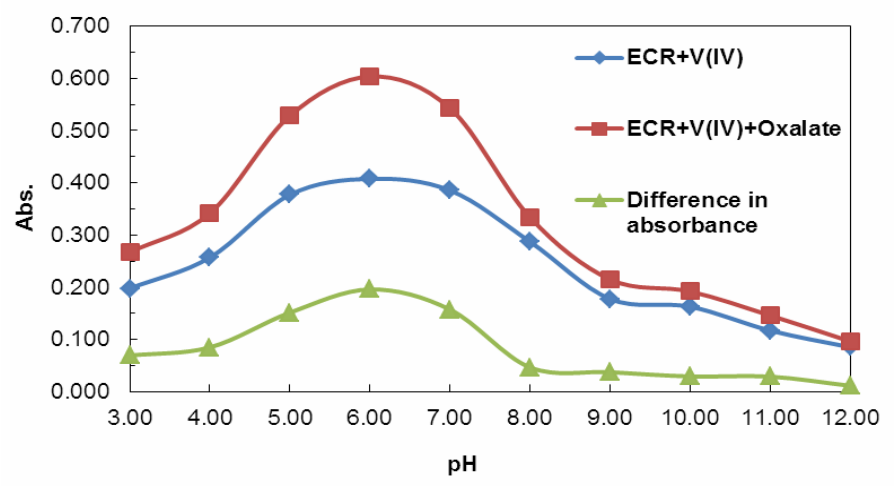

Fig. 2. Absorption spectrum of ECR, ECR-V(IV) and ECR-V(IV)-Ox at 530 nm for different pHs in the room temperature. The concentrations of ECR, V(IV) and Ox solution are 5.0×10^{-4} M, 5.0×10^{-4} M and 8.73×10^{-5} M, respectively.

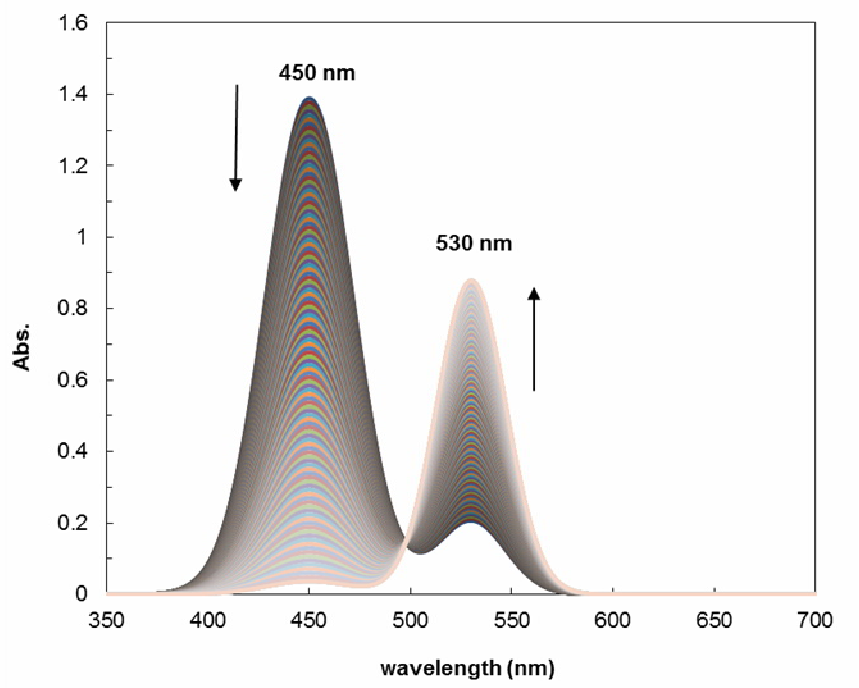

Fig. 3. Absorption behavior of Eriochrome cyanine R in the presence of vanadyl (0-8.33×10^{-5} M) at pH = 6.00, wavelength range between 350-700 nm and in the room temperature.

pH, the protonation of the anionic dyes such as ECR decreases the sensitivity and absorption intensity. On the other hand, since the oxalic acid is formed at lower pHs, the concentration of free oxalate ions is low, leading to a low UV-Vis signal at acidic pHs. At higher pH values, the absorption intensity of the complex decreases. This is likely

due to the competition between hydroxide ions and ligand for complexation with vanadyl ions [37,38].

Spectral Behavior of ECR-vanadyl Complex

The complexation of ECR with VO^{2+} ions causes a bathochromic absorbance shift from 450 to 530 nm which is accompanied by a color change from yellow to purple. 300.0 µl of ECR 5.00×10^{-4} M was added to 3.0 ml of buffer solution of ammonium acetate (pH 6.00). The adduct was transferred to the quartz cell. Afterward, 0.0 to 600.0 µl vanadyl ions (5.00×10^{-4} M) were added to this solution stepwise. After about two minutes for solution equilibration, the absorption spectra were recorded after each addition in the wavelength range of 350.0-700.0 nm.

The spectra showed the increase in the Vanadyl concentration ($0.00\text{-}7.69 \times 10^{-5}$ M), resulting in a decrease in the ECR maximum absorption at 450.0 nm and simultaneous increase in the intensity of the new absorption peak at 530.0 nm (red shift, $\Delta\lambda = 80$ nm), associated with a distinct color change of the probe (yellow to purple), signifying formation of ECR-V(IV) complex (Fig. 3). From the calibration curve of ECR-V(IV) complex at 530.0 and 450.0 nm, the corresponding linear range was obtained between 8.16×10^{-5} M and 8.32×10^{-7} M (Figs. 4 and 5). Also, the formation constant of the ECR-VO^{2+} complex was evaluated to be 1.36×10^{6} from its binding curve. Based on the Job's plot, the stoichiometric ratio of ECR-VO^{2+} complex was suggested as a 1:1 binding mode. This binding mode is in agreement with the previous research studies (Fig. 6) [35].

Spectrophotometric Titration of ECR-V(IV) Complex with Oxalate

By adding oxalate ions to the complex solution (ECR-VO^{2+}), the solution color is changed to yellow, and the absorption peak at 530.0 nm was faded with increasing absorption peak at 450.0 nm due to the release of ECR into the solution. This phenomena refers to the displacement of the indicator from the receptor by analyte because of the stronger formation constant of VO^{2+}-Ox complex.

For the determination of the stability constant of the complex, using a calibrated micropipette, a certain volume of 0.0 to 895.0 µl of oxalate solution (5.00×10^{-4} M) was gradually added to the cuvette solution (containing 3.0 ml ammonium acetate buffer solution pH 6.00, 300.0 µl ECR 5.00×10^{-4} M and 300.0 µl vanadyl 5.00×10^{-4} M). Afterward, the visible spectra of the solution were recorded at 350-700 nm after 2 min equilibrium time (Fig. 7).

According to Fig. 7, the addition of oxalate to the cell causes a decrease in absorbance peak at 530 nm and simultaneously increases the absorption peak at 450 nm. Also, adding oxalate ions produces a very noticeable color change (purple to yellow) which is visible by the naked eyes. Thus, this designed chemosensor is called naked eye chemosensor. From the titration curve of ECR-VO^{2+} solution with oxalate ions, the changes in the maximum absorption of the ECR (450.0 nm) or peak absorption of the ECR-VO^{2+} complex solution (530.0 nm) were plotted against the concentration of the oxalate ions. The calibration curve was obtained from the linear section of the binding curve, which can be used for quantitative determination of oxalate ions and the association constant of the VO^{2+}-Ox complex solution [39]. A linear range for oxalate determination was found to be 8.32×10^{-7} M to 1.24×10^{-4} M at 530.0 nm and 8.32×10^{-7} M to 1.13×10^{-4} at 450.0 nm (Figs. 8 and 9, respectively). Detection limit of this assay method for determination of oxalate ion was obtained to be 5.40×10^{-7} M.

The Stoichiometric Study

The plot of changes in the UV-Vis spectra as a function of the oxalate concentration was fitted with the 1:2 (oxalate:vanadyl) binding model which was confirmed by the Job's plot (Fig. 10). The Job's method was applied to obtain a stoichiometric ratio between vanadyle and oxalate in the mixture of oxalate and ECR-vanadyl complex in which each of them was 5.00×10^{-4} M. The ECR-vanadyl complex solution and oxalate solution were mixed at different volumes (total volume was constant) in the quartz cell containing ammonium acetate buffer at pH = 6.00, and the UV-Vis spectrum was recorded for each volume. Plotting the corrected absorption against the mole fraction of oxalate (Job's plot) showed a maximum at about 0.33 which offers a 1:2 (oxalate:vanadyl) binding stoichiometric ratio for the oxalate-vanadyl complex (Fig. 10).

H NMR Spectroscopy

H NMR study of the indicator, the designed sensor and

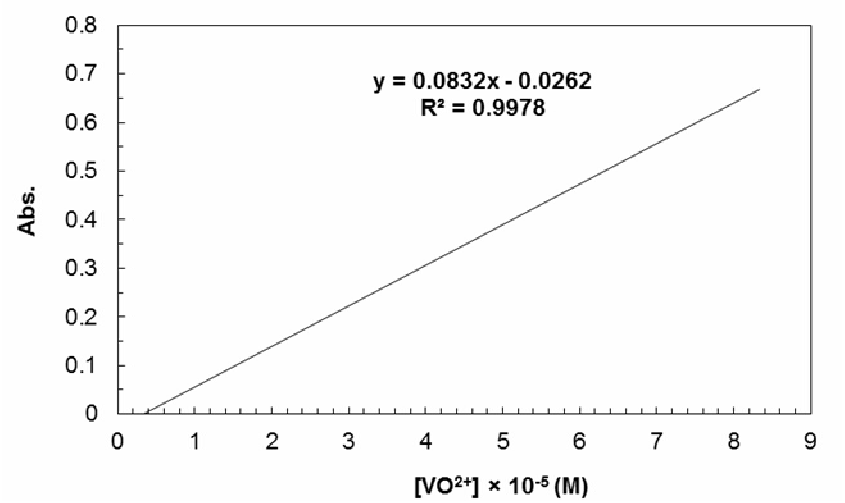

Fig. 4. Calibration curve of ECR-V(IV) at 530 nm, pH = 6.00 and in the room temperature, linear range: 8.32×10^{-7}- 8.16×10^{-5} M.

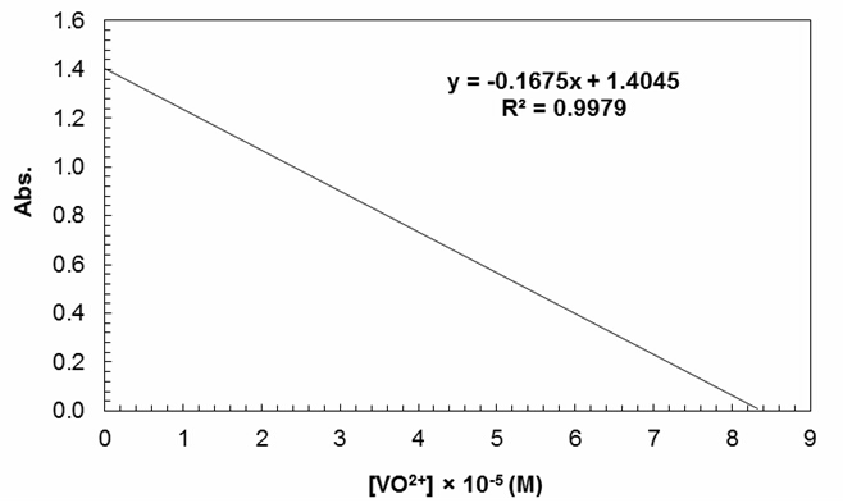

Fig. 5. Calibration curve of ECR-V(IV) at 450 nm, pH = 6.00 and in the room temperature, linear range: 8.32×10^{-7}- 8.16×10^{-5} M.

the product of its interaction with oxalate ion was performed in DMSO at 25 °C. The peak from 2.17 to 2.52 ppm is related to the protons of the methyl group on the cyclo-ketone ring and the aromatic ring. The peak in the range of 7.372-7.463 ppm is related to the protons of the -CH= group in the phenolic aromatic ring and the aromatic ring with the sulfonic group. The available peak at 15.932 ppm is related to the hydroxyl protons of the Ar-OH in the structure (Figs. 11a and 11b).

In Fig. 12, the H NMR spectrum with the corresponding structure of the sodium oxalate is shown. It is clear that sodium oxalate has no peak in the NMR spectrum because it has no proton. Therefore, due to the hydration in aqueous solution, oxalate ion was converted to its acidic form (oxalic acid). So, due to the presence of two groups of -OH, H NMR spectrum had a peak in the range of 2.104-

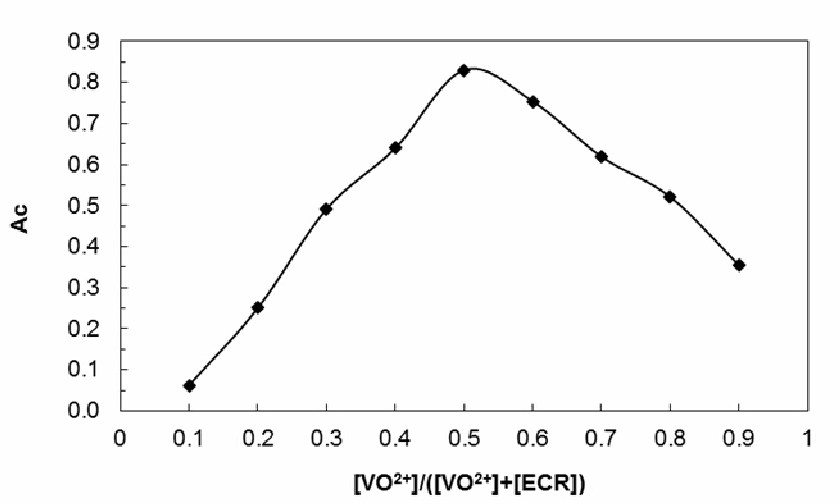

Fig. 6. Job plot of vanadyl and Eriochrome cyanine R complex at pH = 6.00 and 530 nm in the room temperature.

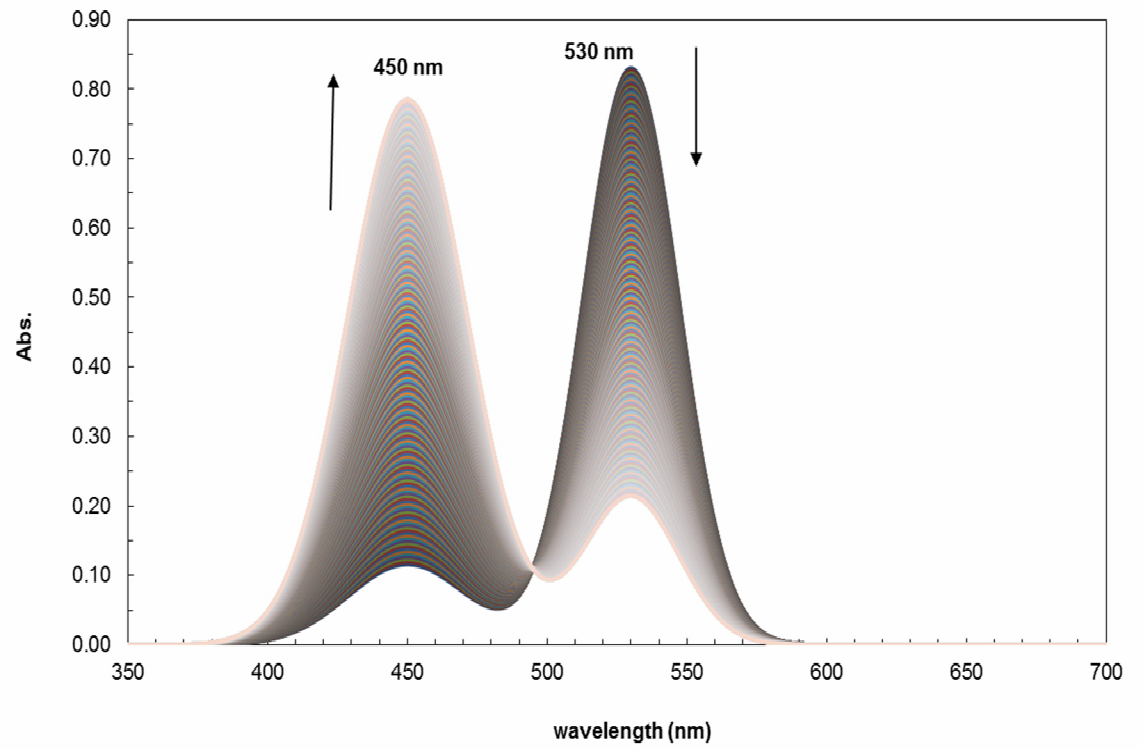

Fig. 7. Change of absorption spectra of ECR-vanadyl complex by adding 0-1.14 × 10^{-4} M oxalate at ammonium acetate buffer (pH = 6.00), wavelength range between 350-700 nm and in the room temperature.

2.869 ppm.

The complex structure and H-NMR spectrum of Eriochrome cyanine R with vanadyl (ECR-VO^{2+}) are shown in Figs. 13a, 13b and 13c. As shown in Figs. 13b and 13c, the peak in the range of 2.060-2.542 ppm is related to protons of the methyl group on cyclo-ketone rings and

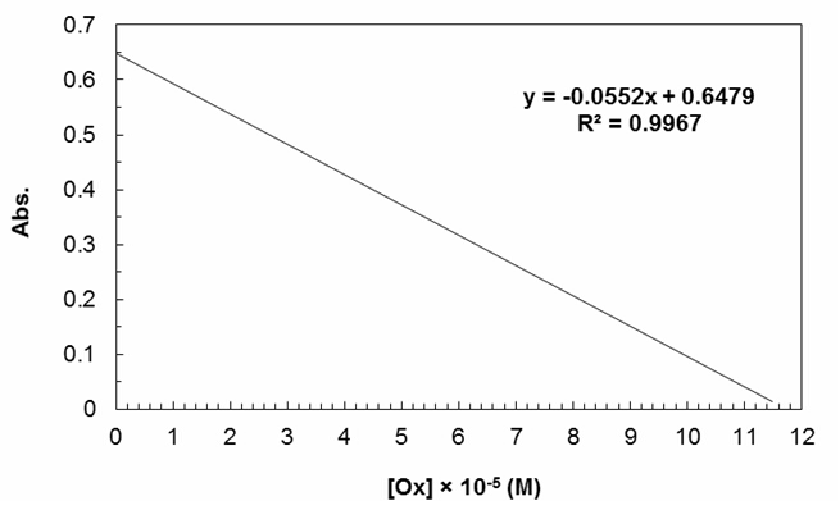

Fig. 8. Calibration curve of ECR-vanadyl complex with oxalate at 530 nm, pH = 6.00 and in the room temperature, linear range: 8.32×10^{-7}-1.24×10^{-4} M.

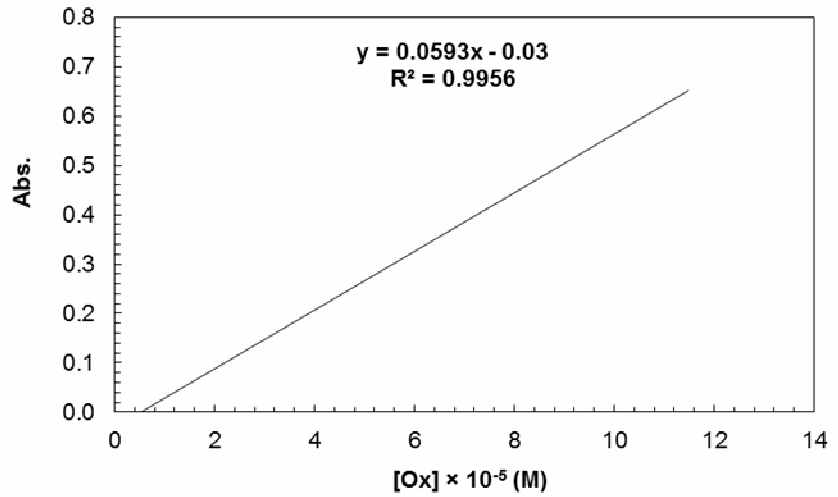

Fig. 9. Calibration curve of ECR- vanadyl complex with oxalate at 450 nm, pH = 6.00 and in the room temperature, linear range: 8.32×10^{-7}-1.13×10^{-4} M.

aromatic rings within the structure of the complex. The peak from 6.639 to 7.205 ppm is related to the protons of the -CH= group in the phenolic aromatic ring and the protons in the cyclo-ketone ring. The peaks in 7.619 and the range of 7.860-8.289 ppm are related to the protons of the -CH= group of the phenolic aromatic ring and the aromatic ring containing sulfonic group. The peak at 15.932 ppm is related to the protons of the phenolic hydroxyl group of the structure.

Comparing Fig. 13b and 13cshows that all chemical shifts of the ligand (ECR) are observed in the complex (ECR-VO^{2+}) spectrum completely, indicating successful synthesis of the complex. The second reason for this complexation is shifting of the chemical shifts. Figures 14a and 14b show the structure of the oxalate-vanadyl complex and its spectrum. As shown in Fig. 14b, the peak in the

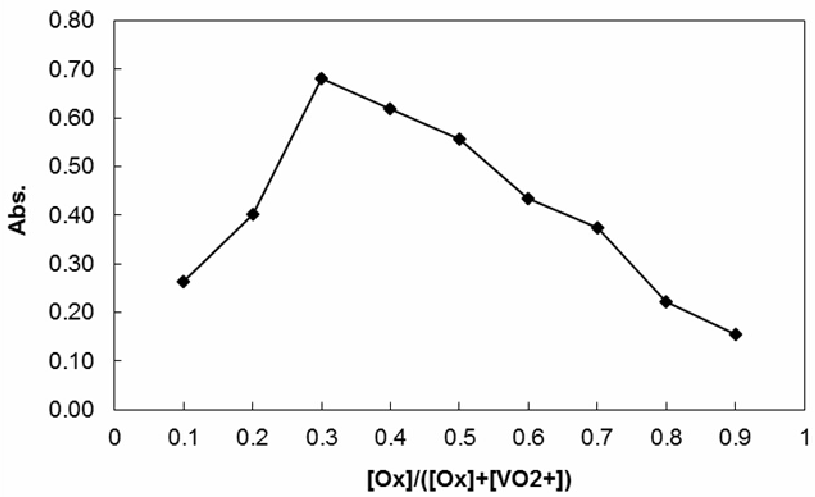

Fig. 10. Job's plot of vanadyl-oxalate at 450 nm, pH = 6.00 and in the room temperature.

range of 2.347-2.690 ppm is related to the hydroxyl group protons in the oxalate-vanadyl complex structure. Comparison Figs. 12 and 14b indicates shifting in chemical shifts due the successful synthesis of the complex. Figures 15a and 15b show the structure of the ternary complex and its spectrum. As seen in the spectrum, the peak in the range of 2.043-2.532 ppm is assigned to the protons of the methyl group on cyclo-ketone rings and aromatic rings within the complex structure. The peak from 6.611 to 7.495 ppm is related to the protons of the -CH= group in the phenolic aromatic ring and the cyclo-ketone ring.

The peaks at 7.605 and the range from 7.831-8.285 ppm are related to the protons of the -CH= phenolic aromatic ring and the aromatic ring containing the sulfonic group. Comparison of the chemical shifts of the ECR-VO^{2+} complex with those of a ternary complex of ECR-VO^{2+}-Ox shows that the spectral numbers in Figures 13c, 14b and 15b are similar and the variation in these chemical shifts reflects their differences, suggesting their successful synthesis.

The Sensor Repeatability

The repeatability of the designed sensor implicates its precision. To evaluate the repeatability of the sensor, five sensors were prepared in the vial in the same conditions and oxalate solution was added to them, so that the concentration of the oxalate in the cell reached 8.73×10^{-5} M. To assess the accuracy of the method, the absorbace of these mixtures at 450.0 nm was recorded by the spectrophotometer. The variation coefficient of the sensor response as a precision criterion was calculated to be 0.52% (Fig. 16).

Response Time

One of the important characteristics of the sensor is fast response time. The response time is the time required for the indicator displacement by the analyte for binding to the receptor as its color turns yellow (ECR is released). So, absorption changes of adding oxalate ions (8.73×10^{-5} M) to the chemosensor (ECR-VO^{2+} complex) were recorded at λ_{450} and λ_{530} within 250 s in time course mode of spectrophotometer. According to the recorded spectra, the solution had the most absorption changes within 70 s and after that no significant changes are obsereved; thus, the equivalent time for the oxalate ions interaction is 70 s. These results show the fast reaction of vanadyl and oxalate leading to the fast response of the sensor for the oxalate determination (Fig. 17).

Selectivity

To study the selectivity of the chemosensor, it was mixed with various anions, including HCO_3^-, CO_3^{2-}, Br^-, Cl^-, F^-, I^-, NO_3^-, $H_2PO_4^-$, PO_4^{3-}, ClO_4^-, IO_3^-, N_3^-, NO_2^-, NO_3^-, SCN^-, SO_3^-, $P_2O_7^{4-}$, $Cr_2O_7^{4-}$, ClO_3^-, BrO_3^-, IO_3^-, $S_2O_3^{2-}$ and citrate. Thus, the interaction of ECR (8.73×10^{-5} M)-VO^{2+}

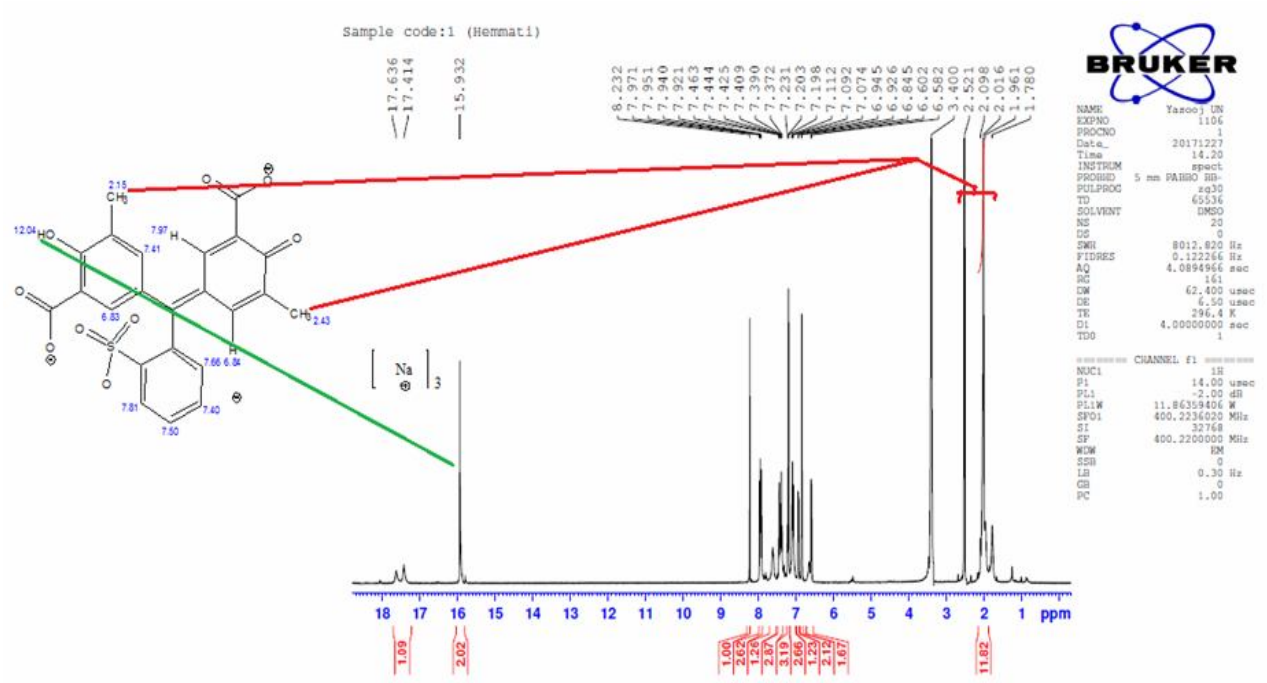

(a)

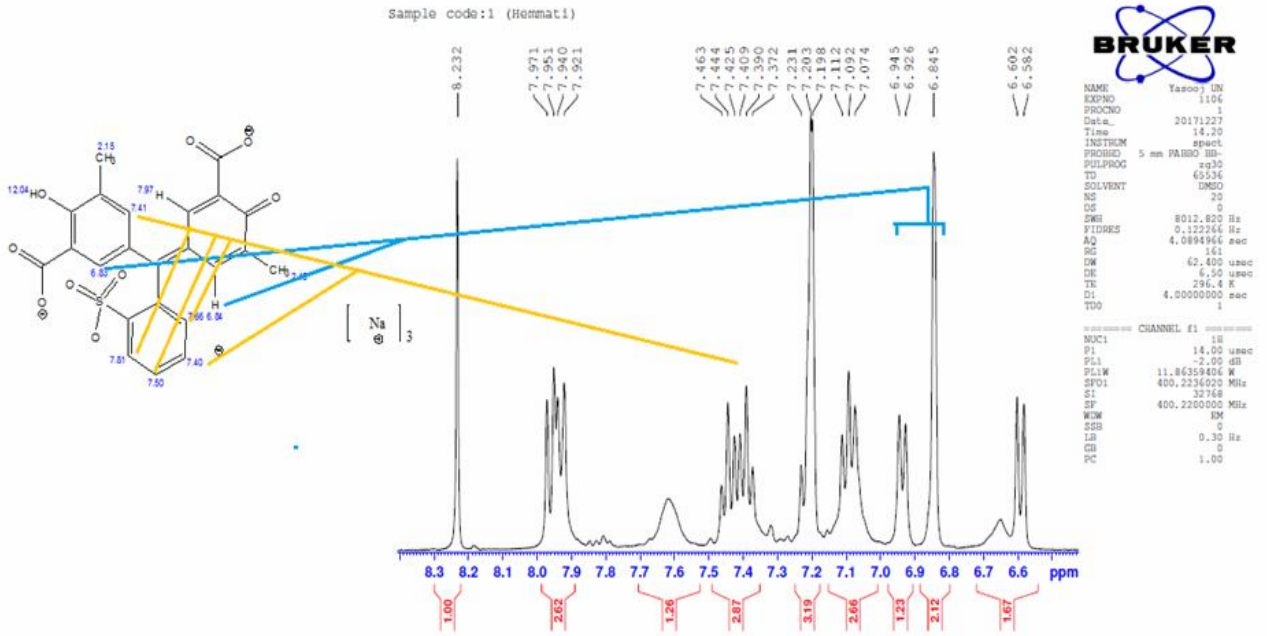

(b)

Fig. 11. a) H NMR spectrum of Eriochrome cyanine R; b) H NMR spectrum of Eriochrome cyanine R (6.5-8.3 ppm) in DMSO.

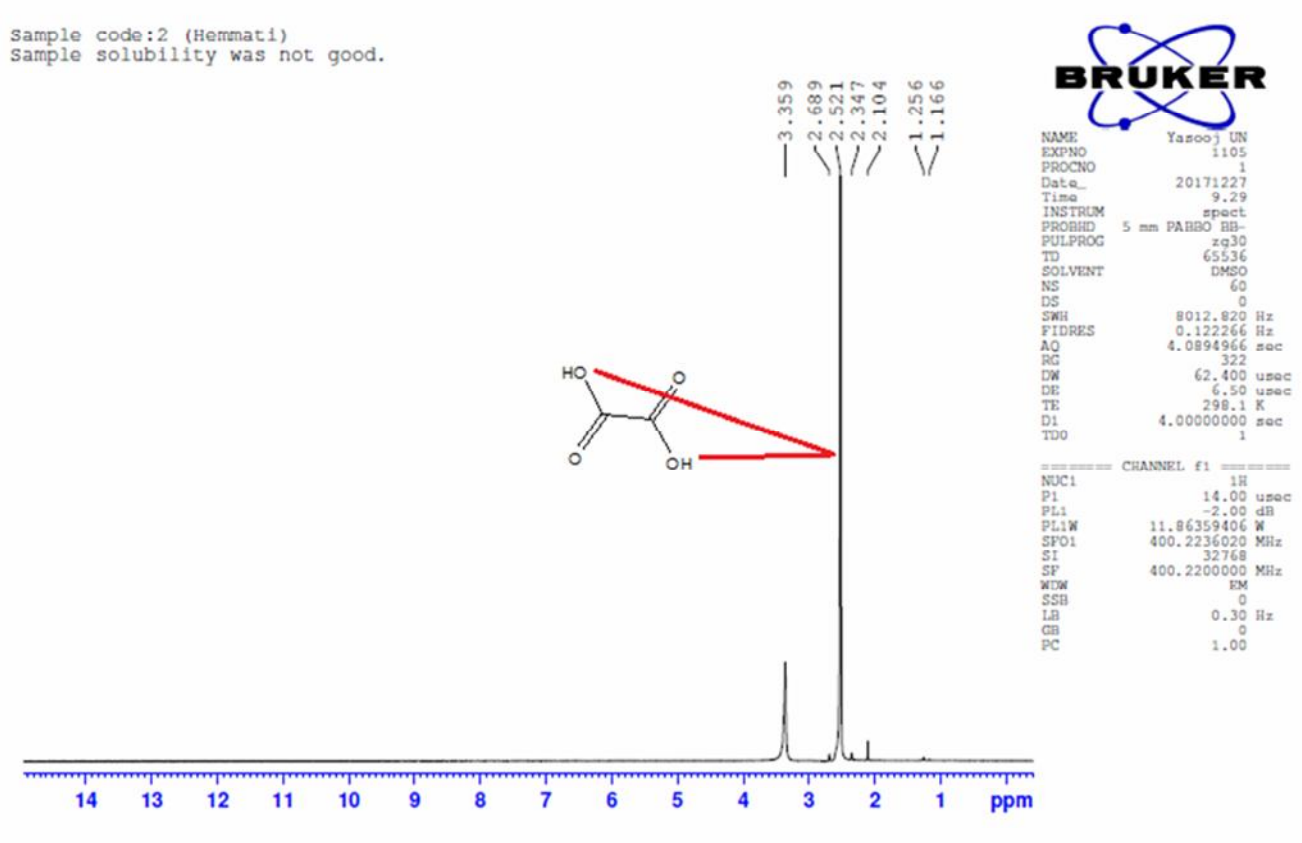

Fig. 12. H NMR spectrum of sodium oxalate in its acidic form (oxalic acid) in DMSO.

(5.00×10^{-4} M) complex with each of the mentioned anions (8.73×10^{-5} M) in ammonium acetate buffer solution at pH 6.00 was studied. The spectrophotometer recorded the absorption of the mixture solution (ECR-VO^{2+} and anions) at λ_{530}. It was seen that the addition of anions to the ECR-VO^{2+} complex solution did not result in any significant change in the absorption band (did not affect the color of the ECR-VO^{2+} solution), suggesting that the interactions of the ECR-VO^{2+} complex with these anions are not strong or the anions do not react with vanadyl ions. Thus, only oxalate ions promote significant changes in the absorption intensity and also in the amount of A_{450}/A_{530} (Fig. 18). Therefore, the ECR-VO^{2+} complex is very useful for the simple selective sensing of the oxalate ions by a color change at a very low concentration in water.

Applications

Five human urine samples were prepared, and certain amounts of oxalate ions were added to each of these samples with three replicates for each of them. The proposed sensor determines the oxalate content of the samples. So, the percentage of the recovery and relative standard deviation (RSD) were calculated for three measurements in each of the urine samples. The recoveries were between 96 and 106% with acceptable precision (RSD < 0.05) (Table 2). These results indicated the applicability and reliability of the designed sensor in the quantitative determination of oxalate ions in real samples.

For the miniaturization of the sensor response over different conditions, the logic gate behavior of this IDA system was designed using vanadyl and oxalate ions as input and UV-Vis absorbance signal of ECR at 450.0 nm output. The presence and absence of vanadyl or oxalate ions were considered to be "1" and "0" states, respectively. Only in the presence or absence of both oxalate and vanadyl ions in the solution, the UV-Vis signal at λ_{450} is high or logic

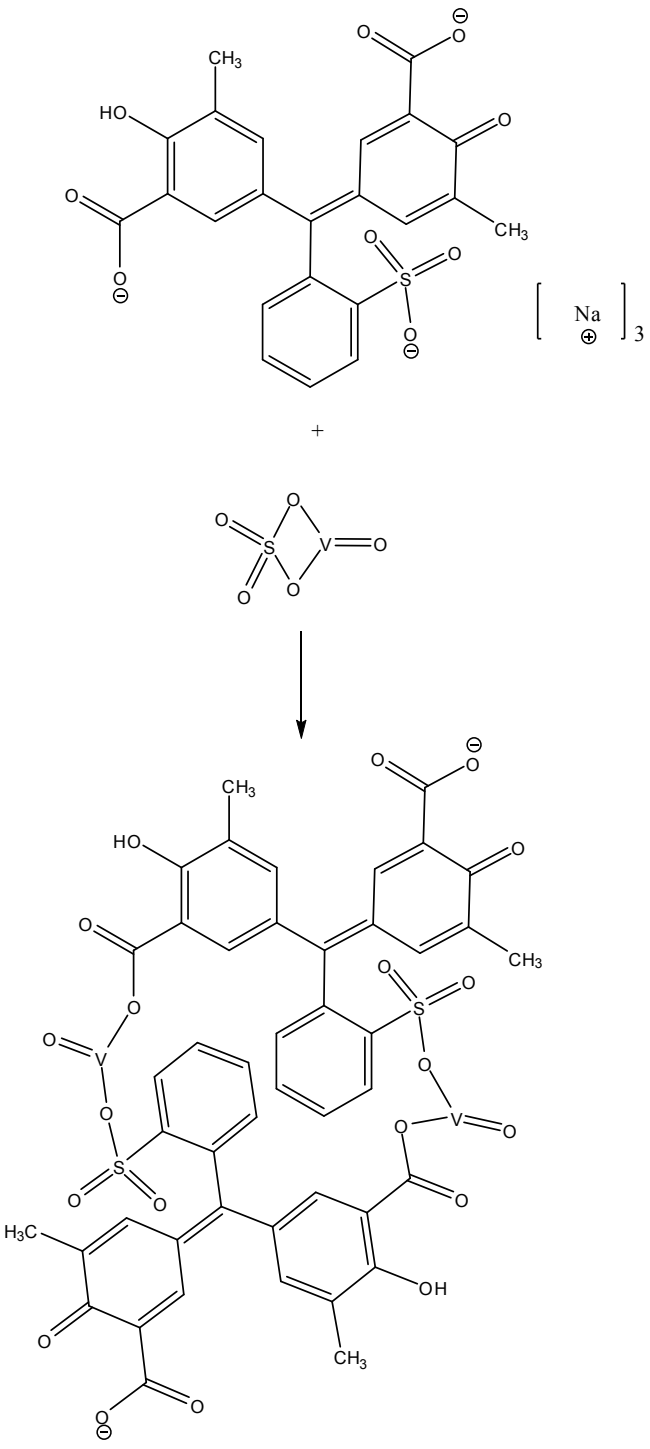

(a)

Fig. 13. a) Structure of ECR-VO^{2+} complex in DMSO; b) H NMR spectrum of ECR-VO^{2+} complex with corresponding chemical shift; c) H NMR spectrum of ECR-VO^{2+} complex with corresponding chemical shift.

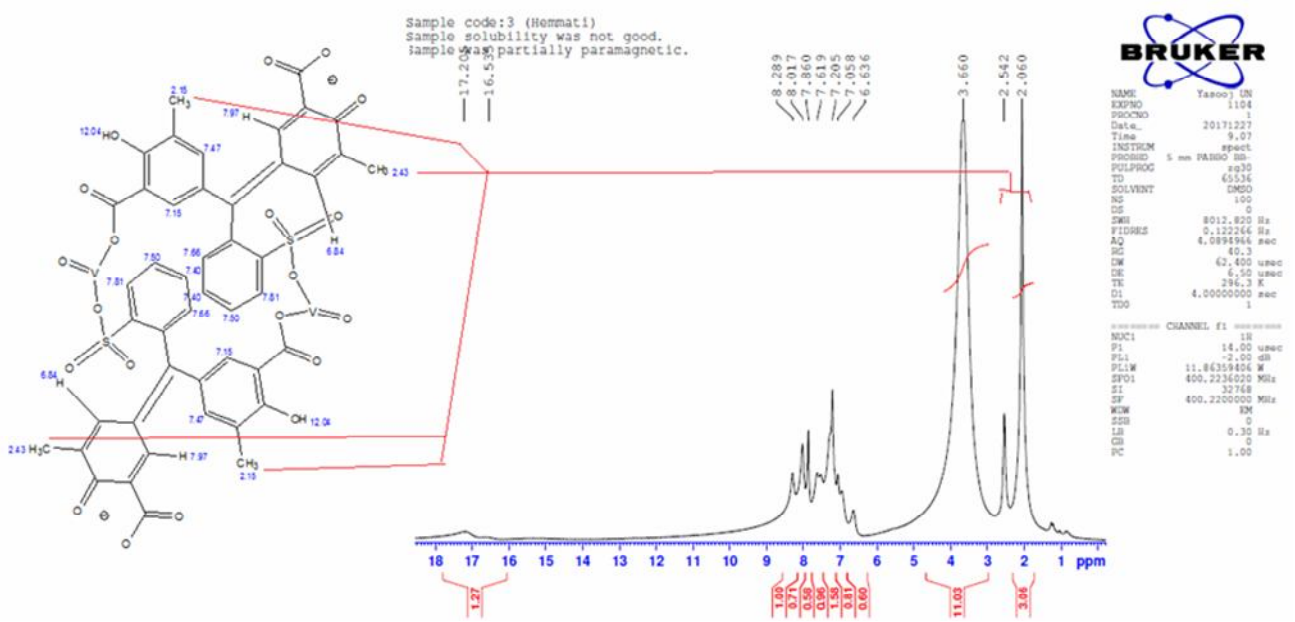

(b)

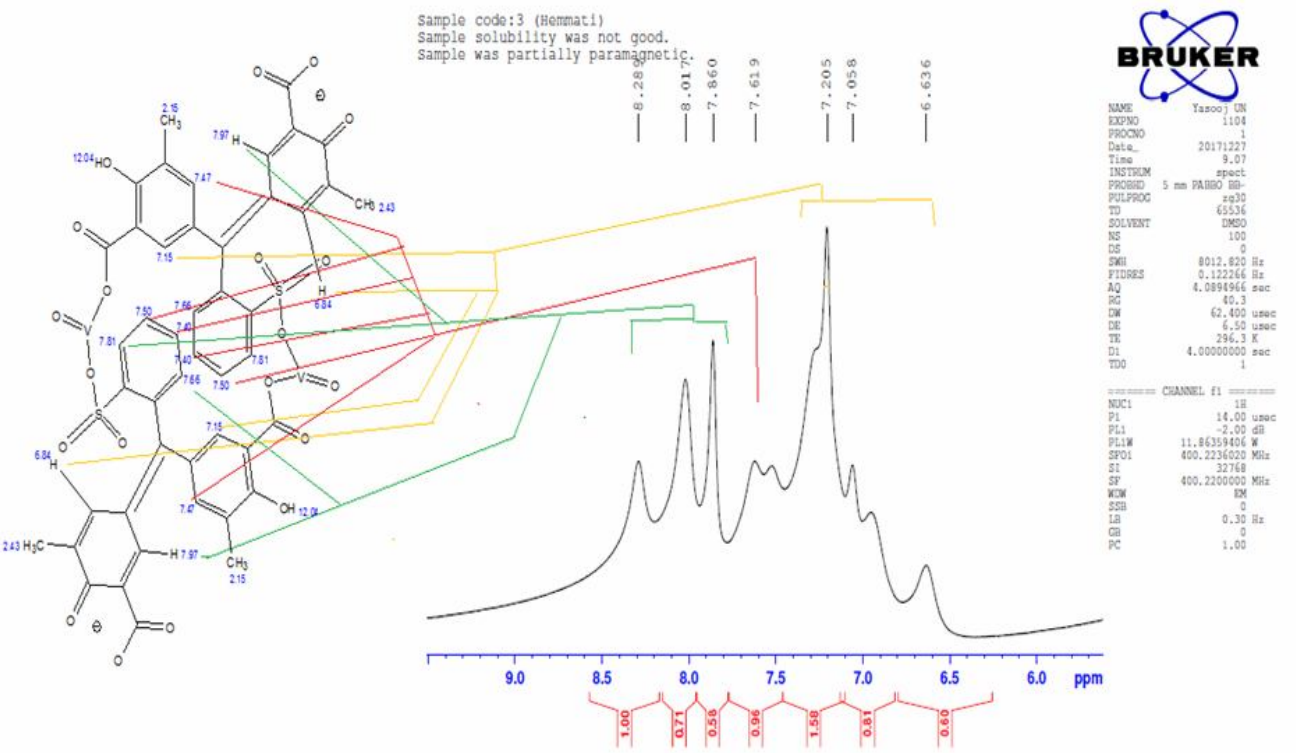

(c)

Fig. 13. Continued.

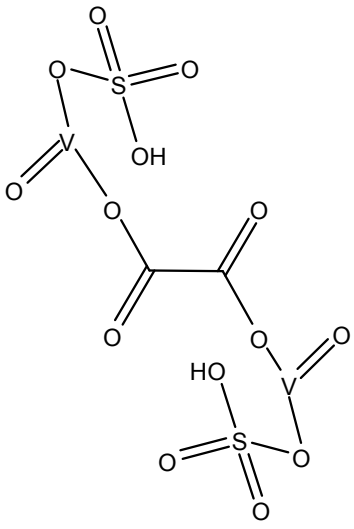

(a)

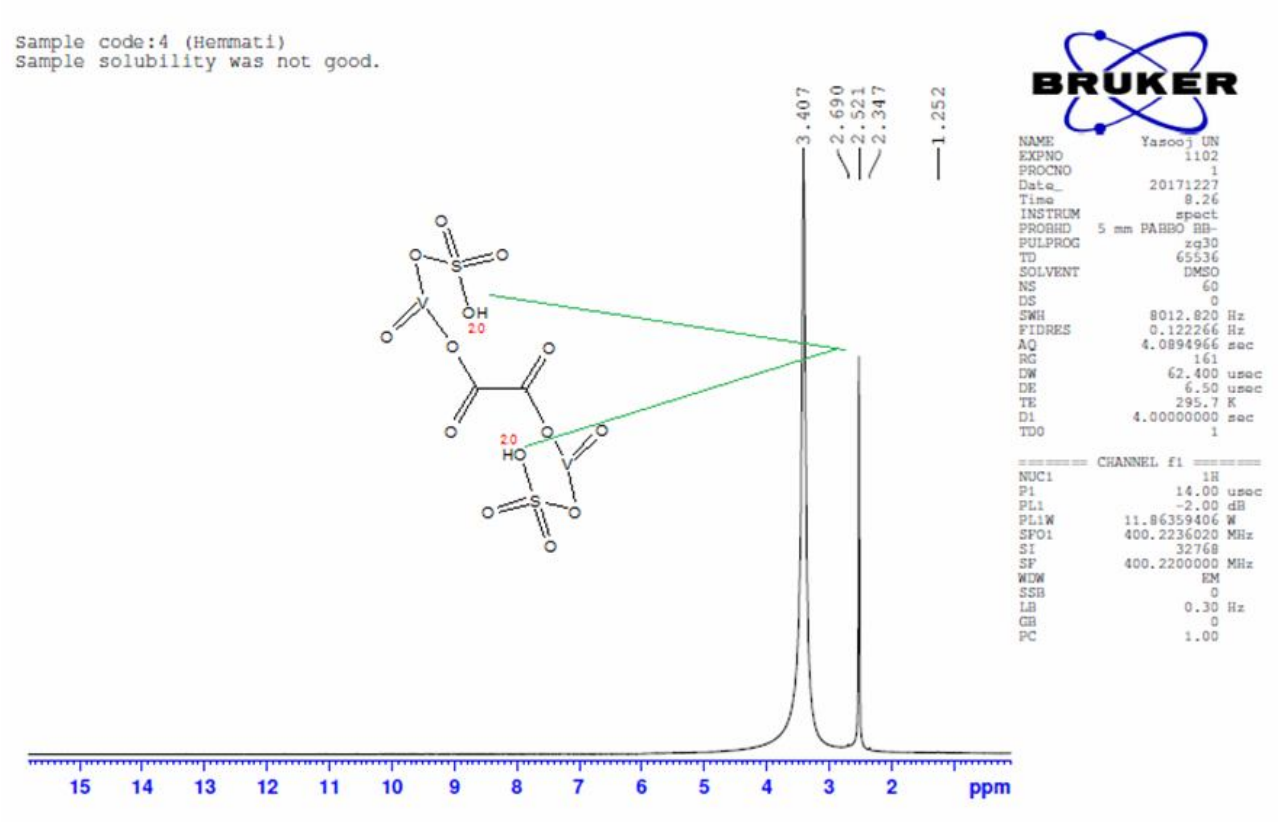

(b)

Fig. 14. a) Oxalate-vanadyl complex structure; b) The H NMR spectrum of oxalate-vanadyl complexes and their respective chemical shift.

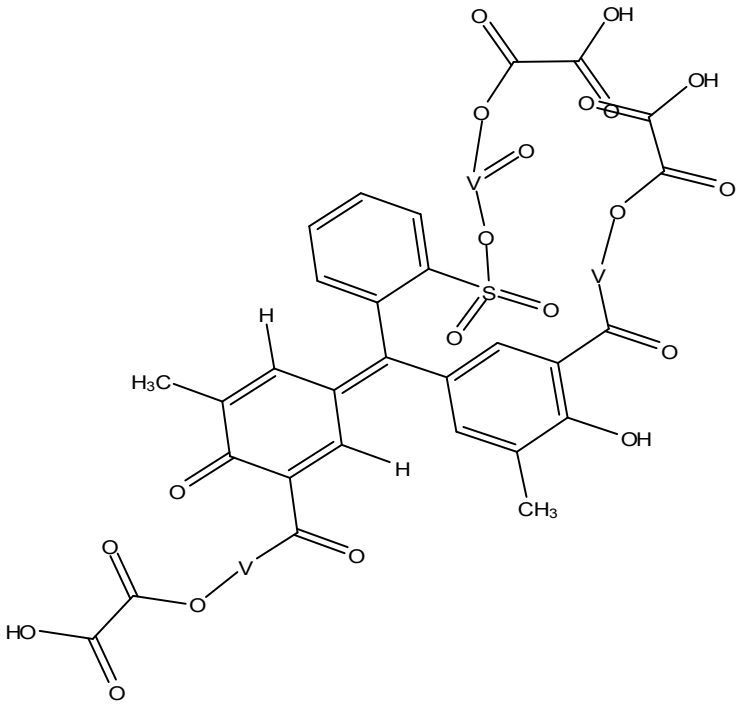

(a)

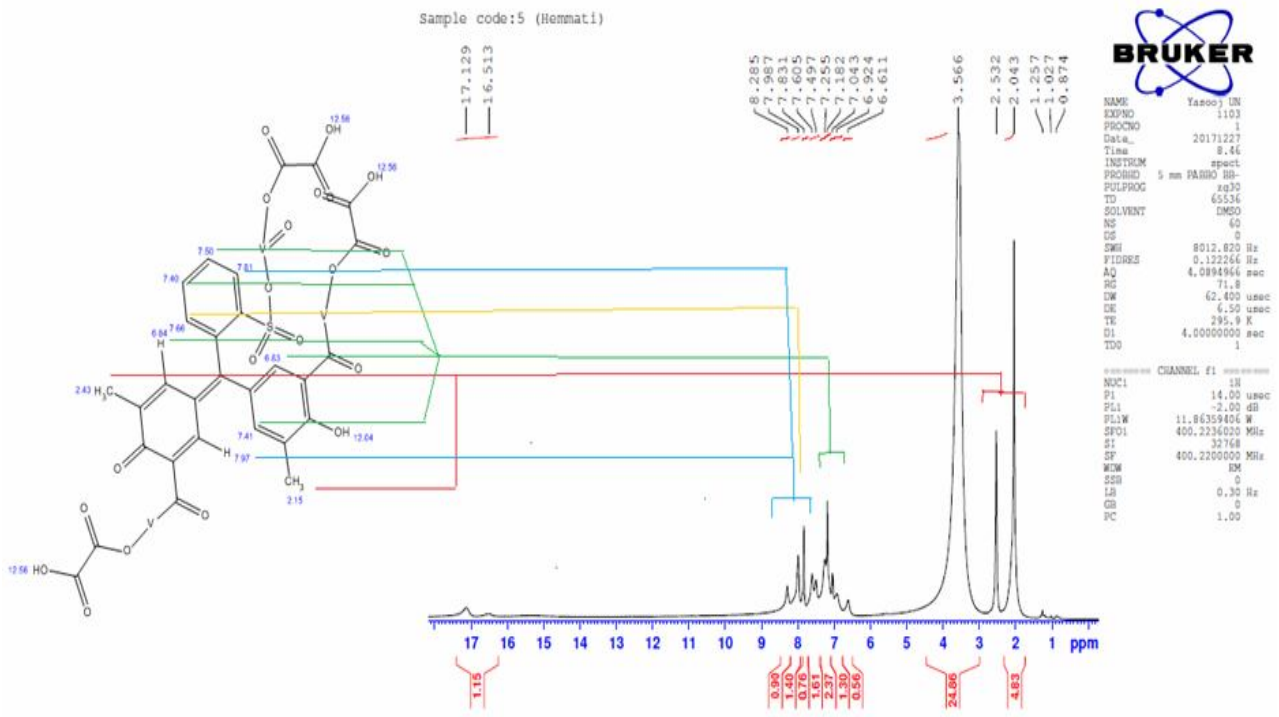

(b)

Fig. 15. a) The ternary complex structure of ECR-VO^{2+}-Ox; b) The ternary complex spectrum of ECR-VO^{2+}-Ox.

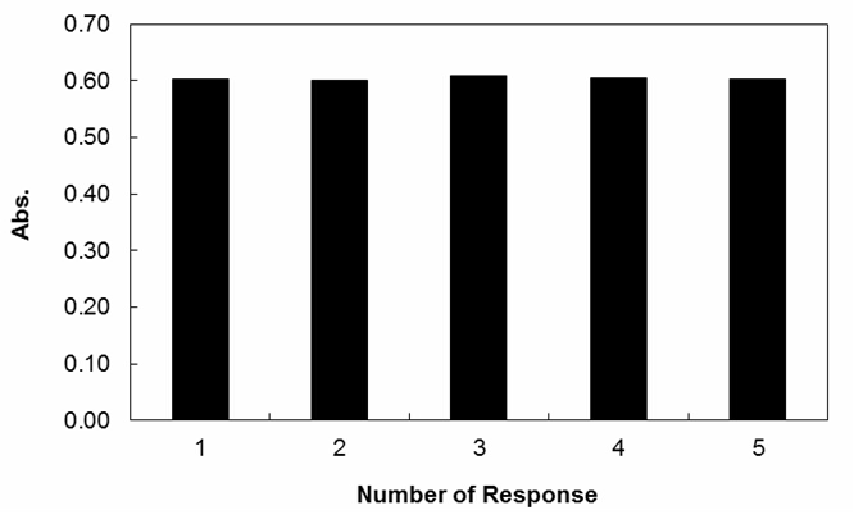

Fig. 16. Repeatability of designed chemosensor for five replicated determinations of oxalate at optimum conditions (pH = 6.00 and in the room temperature).

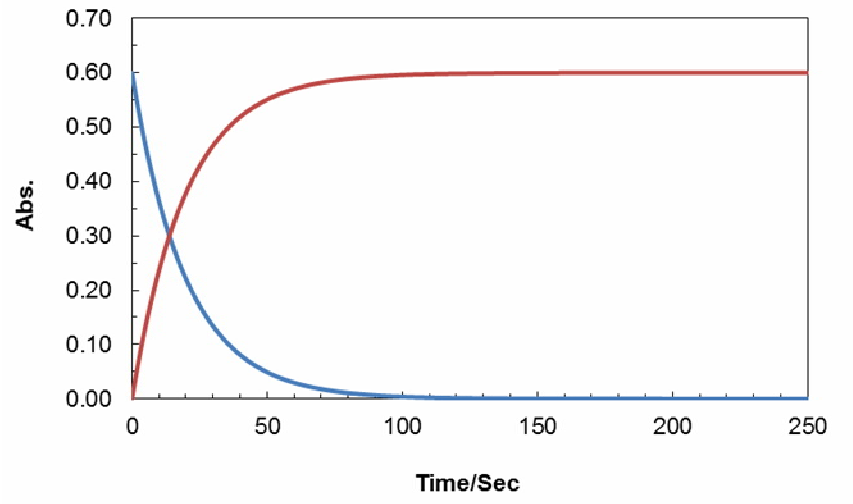

Fig. 17. Response time study with addition of 8.73×10^{-5} M oxalate to complex at 450 nm (red) and 530 nm (blue). The experiment was done in optimum conditions (pH = 6.00 and in the room temperature).

gate state is "1". So, the mode of logic gates of the sensor is XNOR. The corresponding truth table and scheme of this logic gate are shown in Table 3 and Fig. 19. The ability of the proposed sensor for determining oxalate was compared with the other analytical approaches which are shown in Table 4. As can be seen, the sensitivity of the proposed method is better than the previous analytical methods.

CONCLUSIONS

According to the above results and previous reports on detection and determination of oxalate ions, a new simple colorimetric probe was designed for the detection and determination of oxalate ions in some real samples. Using the chemosensor, the qualitative and quantitative

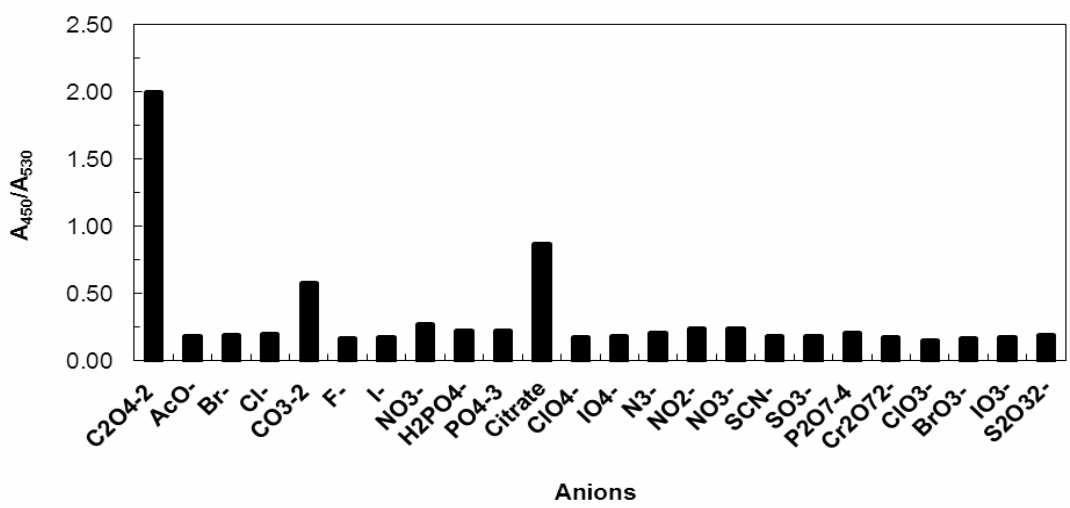

Fig. 18. The response of the ECR-VO^{2+} (5×10^{-4} M) system upon the addition of oxalate and other anions (8.73×10^{-5} M) in ammonium acetate buffer at 530 nm, pH = 6.00 and in the room temperature.

Table 2. Analytical Results of Oxalate in Real Samples

Urine sample	Oxalate content (M)		Recovery
	Added	Founded[a]	
Sample 1	-	-	-
Sample 2	1.22×10^{-5}	$1.29 \times 10^{-5} \pm 0.035$	105.73
Sample 3	4.13×10^{-5}	$3.98 \times 10^{-5} \pm 0.029$	96.36
Sample 4	6.20×10^{-5}	$6.06 \times 10^{-5} \pm 0.032$	97.74
Sample 5	7.92×10^{-5}	$8.01 \times 10^{-5} \pm 0.037$	101.13

[a]Average of three determinations ± S.D.

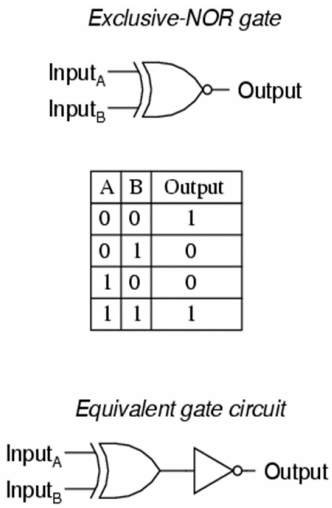

Fig. 19. Corresponding logic scheme for XNOR with its truth table.

Table 3. Comparison of the Oxalate Determination in Urine Samples with Different Methods

Method	Response time	Linearity range (M)	LOD	RSD (%)	Ref.
Paper-based colorimetric method	300 s	1×10^{-5}-1×10^{-3}	1×10^{-5} M	8%	[46]
OXD-CO_2, sensing electrod	480-600 s	2×10^{-4}-1×10^{-2}	4×10^{-5} M	4.52%	[47]
TiO_2-FeNPs/CILE	-	5.00×10^{-5}-3.00×10^{-3}	2.31×10^{-5} M	3.2%	[48]
Catalase model compound with	600 s	2×10^{-6}-2×10^{-5}	2×10^{-6} M	3.74%	[49]
Oxalate oxidase	1200 s	5×10^{-5}-1×10^{-3}	5×10^{-5} M	1.89%	[50]
Ion chromatography	70 s	8.30×10^{-7}-1.13×10^{-4}	8.32×10^{-7} M	0.52%	Proposed
IDA					method

Table 4. The Truth Table for XNOR Logic Gate of the Chemosensor

Input A (V(IV))	Input B (Oxalate)	Output (Color intensity of ECR at 450 nm)
0	0	1
0	1	0
1	0	0
1	1	1

determination of oxalate was characterized by a color change from purple to yellow (naked eyes) accompanied by about 80 nm blue shifts. The measurement of the oxalate ions with this chemosensor (ECR-Vanadyl) has a limit of detection of 5.40×10^{-7} M. Therefore, the oxalate concentration was determined with high precision by this chemosensor because of the appropriate linear range and good detection limit. Selectivity tests have shown that other anions do not interfere with the detection and determination of oxalate by the sensor, so, the designed chemosensor has good selectivity. The related logic gate of this process is shown in terms of XNOR logic gates.

REFERENCES

[1] S. Milardović, I. Kereković, M. Nomkdilo, Talanta 77 (2008) 222.

[2] M.D.L. de Castro, J. Pharm. Biomed. Analysis 6 (1988) 1.

[3] A. Hodgkinson, A. Williams, Clin. Chim. Acta 36 (1972) 127.

[4] E.J. O'Neil, B.D. Smith, Coord. Chem. Rev. 250 (2006) 3068.

[5] J. Chen, Q. Lin, Q. Li, W.T. Li, Y.M. Zhang, T.B. Wei, RSC Adv. 6 (2016) 86627.

[6] H. Khajehsharifi, M.M. Bordbar, Sens. Actuators, B: Chem. 209 (2015) 1015.
[7] R.E. Neas, J.C. Guyon, Anal. Chem. 44 (1972) 799.
[8] A.D. Britton, J.C. Guyon, Anal. Chim. Acta 44 (1969) 397.
[9] R. Bais, N. Potezny, I.B. Edwards, A.M. Rofe, A.J. Conyers, Anal. Chem. 52 (1980) 508.
[10] A.L. Allan, B.S. Fernandez Band, E. Rubio, Microchem. J. 34 (1986) 51.
[11] P. Nuret, M. Offner, Clin. Chim. Acta 82 (1978) 9.
[12] P.C. Hallson, G.A. Rose, Clin. Chim. Acta 55 (1974) 29.
[13] M.F. Laker, A.F. Hafmann, B.J.D. Meeuse, Clin. Chem. 26 (1980) 827.
[14] A. Ichiyama, E. Nakai, T. Funai, T. Oda, R. Katafuchi, J. Biochem. 98 (1985) 1375.
[15] S. Imaoka, Y. Funae, T. Sugimoto, N. Hayahara, M. Maekawa, Anal. Biochem. 128 (1983) 459.
[16] J. Zerwekh, E. Drake, J. Gregory, *et al*., Clin. Chem. 29 (1983) 1977.
[17] M. Toyoda, Urol. Res. 13 (1985) 179.
[18] R.P. Singh, G.H. Nancollas, Anal. Lett. 19 (1986) 1487.
[19] F.E. Cole, K.M. Gladden, D.J. Bennett, D.T. Erwin, Clin. Chim. Acta 139 (1984) 137.
[20] M. Sugiura, H. Yamamura, K. Hirano, *et al*., Clin. Chim. Acta 105 (1980) 393.
[21] C.J. Farrington, A.H. Chalmers, Clin. Chem. 25 (1979) 1993.
[22] N. Potezny, R. Bais, P.D. O'Loughlin, J.B. Edwards, A.M. Rofe, R.A.J. Conyers, Clin. Chem. 29 (1983) 16.
[23] C.S. Pundir, M. Sharma, Sci. Ind. Res. 69 (2010) 489.
[24] H. Tavallali, M.R. Baezzat, G. Deilamy-Rad, A. Parhami, N. Hasanli, J. Lumin. 160 (2015) 328.
[25] H. Tavallali, G. Deilamy-Rad, A. Parhami, N. Hasanli, Spectrochim. Acta A Mol. Biomol. Spectrosc. 139 (2015) 253.
[26] H. Tavallali, G. Deilamy-Rad, A. Parhami, N. Hasanli, J. Hazard. Mater. 266 (2014) 189.
[27] X. Zhao, C.Z. Huang, Analyst 135 (2010) 2853.
[28] G. Wang, H. Chen, Y. Chen, N. Fu, Sens. Actuators, B: Chem. 233 (2016) 550.
[29] X. Tian, X. Guo, F. Yu, L. Jia, Sens. Actuators, B: Chem. 232 (2016) 181.
[30] J. Liu, X. He, J. Zhang, T. He, L. Huang, J. Shen,D. Li, H. Qiu, S. Yin, Sens. Actuators, B: Chem. 208 (2015) 538.
[31] T. Liu, N. Li, J.X. Dong, H.Q. Luo, N.B. Li, Sens. Actuators, B: Chem. 231 (2016) 147.
[32] S. Mukherjee, S. Talukder, J. Lumin. 177 (2016) 40.
[33] A. Aviram, J. Am. Chem. Soc. 110 (1988) 5687.
[34] A.P. de Silva, H.Q.N. Gunaratne, C.P. McCoy, Nature 364 (1993) 42.
[35] M.M. Bordbar, H. Khajehsharifi, A. Solhjoo, Spectrochim. Acta, Part A: Mol. Biomol. Spectroscopy 151 (2015) 225.
[36] H. Khajehsharifi, A. Solhjoo, M.M. Bordbar, Ir. J. Anal. Chem. 3 (2016) 145.
[37] S. Boudra, J.M. Bosque-Sendra, M.C. Valencia, Talanta 42 (1995) 1525.
[38] O. Mortaz Hejri, E. Bzorgzadeh, M. Soleimani, R. Mazaheri, World App. Sci. J. 15 (2011) 218.
[39] A.P. Umali, E.V. Anslyn, J. Chem. Edu. 87 (2010) 832.
[40] S. Burrows, Analyst 75 (1950) 80.
[41] S. Milardovic´, I. Kerekovic, M. Nodilo, Talanta 77 (2008) 222.
[42] C. Merusi, C. Corradini, A. Cavazza, C. Borromei, P. Salvadeo, Food Chem. 120 (2010) 615.
[43] H. Hu, H. Jin, X. Chai, J. Ind. Eng. Chem. 20 (2014) 13.
[44] E.M. Rakhman'ko, Y.V. Matveichuk, L.S. Stanishevskii, V.V. Yasinetskii, J. Anal. Chem. 70 (2015) 873.